



University of Bahrain  
**Journal of the Association of Arab Universities for  
Basic and Applied Sciences**

www.elsevier.com/locate/jaaubas  
www.sciencedirect.com



## تقييم جيوتقني للظروف الأرضية بجوار مبني مائل في مدينة القاهرة – مصر، باستخدام التقنيات الجيوفيزيائية<sup>1</sup>

فتحي شعبان<sup>2,1</sup>، أحمد إسماعيل<sup>2,1</sup>، أسامة مسعود<sup>1</sup>، هاني صلاح<sup>1</sup>، أحمد ليثي<sup>1</sup> وعباس محمد عباس<sup>1</sup>

<sup>1</sup>المعهد القومي للبحوث الفلكية والجيوفيزيقية، حلوان، مصر

<sup>1</sup>المساحة الجيولوجية باليون، جامعة اليون، أمريكا

<sup>2</sup>قسم الفيزياء، كلية العلوم، جامعة الملك خالد، المملكة السعودية العربية

### الملخص:

إن سهل وادي النيل كان مسكنا آمن علي مر التاريخ إلا إنه في الأوان الأخيرة ومع تزايد عدد السكان والتوسع العمراني، بدأت بعض المباني في التعرض لأضرار هيكلية والتي لا تتعلق بتصاميم البناء ولكن بظروف الأرض حول أساسات المباني. إن التغير في خصائص التربة حول المباني مثل قدرة التحمل ومحتوي الرطوبة ربما قد يؤدي إلي انهيار هذه المباني. وتعد هذه الدراسة محاولة لتوصيف التغير في خواص التربة حول مجمع سيتي ستار للتسوق في شرق القاهرة، حيث يتواجد هناك مبنى الكبير يعاني من ميلان ملحوظ أخذ في التزايد عبر السنوات القليلة الماضية، مما قد يؤدي إلى انهيار المبنى بالكامل إذا ما استمر بالميلان بنفس المعدل. وقد تم استخدام التطبيقات الجيوفيزيائية المتكاملة متعددة القنوات بما في ذلك تحليل الموجات السطحية (MASW)، رادار الاختراق الأرضي (GPR) والتصوير المقطعي بالمقاومة الكهربائية (ERT) حول المبنى المتضرر للمساعدة في الكشف عن الأسباب المحتملة للتدهور. وقد أظهرت البيانات الجيورادارية وجود طبقة من التربة تعلق طبقة سميكة عالية الرطوبة، كما إن بيانات (MASW) دلت على وجود طبقة متوسطة لها سرعة موجة قص صغيرة محصورة بين طبقتين لهما سرعة موجة قص كبيرة. في حين أظهر التصوير الكهربائي وجود طبقة جيوكهربية لها مقاومة صغيرة تعلق طبقة لها مقاومة كهربائية كبيرة. أكدت النتائج الجيوفيزيائية مجتمعة وجود تغير أفقي ورأسي في خصائص التربة حول المبنى بحيث يصبح هذا التغير كبير جدا بالقرب من زاوية المبنى المائلة.



University of Bahrain  
**Journal of the Association of Arab Universities for  
Basic and Applied Sciences**

www.elsevier.com/locate/jaaubas  
www.sciencedirect.com



# Geotechnical assessment of ground conditions around a tilted building in Cairo–Egypt using geophysical approaches

Fathy Shaaban <sup>a,c,\*</sup>, Ahmed Ismail <sup>a,b</sup>, Usama Massoud <sup>a</sup>, Hany Mesbah <sup>a</sup>,  
Ahmed Lethy <sup>a</sup>, Abbas Mohamed Abbas <sup>a</sup>

<sup>a</sup> National Research Institute of Astronomy and Geophysics (NRIAG), 11722 Helwan, Egypt

<sup>b</sup> Illinois State Geological Survey, University of Illinois at Urbana-Champaign, USA

<sup>c</sup> Department of Physics, Faculty of Science, King Khaled University, Abha, Saudi Arabia

Received 4 March 2012; revised 22 June 2012; accepted 23 June 2012

Available online 28 July 2012

## KEYWORDS

Multi-channel analysis of surface wave;  
Ground penetrating radar;  
Electrical resistivity tomography;  
Geotechnical investigation;  
Greater Cairo;  
Egypt

**Abstract** The flood plain of the Nile River has been a safe dwelling throughout history. Recently with a growing population and vast growing urbanization some buildings have started to experience structural damages, which are not related to their construction design, but rather to the ground conditions around the buildings' foundations. Variations in properties of the soil supporting the buildings' foundations such as soil bearing capacity, moisture content and scouring may eventually lead to the failure of these buildings. This study is attempting to characterize the variations in the soil properties around the City Star shopping mall, in eastern Cairo, where a large building has tilted over the past few years. This tilting may lead to the collapse of the whole building if it continues at the same rate. An integrated geophysical investigation including multi-channel analysis of surface wave (MASW), ground penetrating radar (GPR) and 2-D electrical resistivity tomography (ERT) was used around the affected building to help detect possible causes of deterioration. The GPR data showed a soil-fill layer overlaying a thick bottom layer of higher moisture content. The MASW data revealed a middle layer of relatively low shear wave velocity sandwiched between two relatively high shear wave velocity layers. The ERT data showed an upper low resistivity layer overlying a high resistivity layer. Integrating the interpretations of the three geophysical methods provide a combined model that reflects lateral and vertical variation in the soil properties. This variation becomes dramatic near the tilted corner of the building.

© 2012 University of Bahrain. Production and hosting by Elsevier B.V. All rights reserved.

\* Corresponding author at: National Research Institute of Astronomy and Geophysics (NRIAG), 11722 Helwan, Egypt.

E-mail address: shaaban\_F@hotmail.com (F. Shaaban).

Peer review under responsibility of University of Bahrain.



Production and hosting by Elsevier

## 1. Introduction

Using non-invasive geophysical techniques for near surface characterization of geotechnical sites has grown rapidly during the last few decades as information derived from borings has become costly. Geophysical techniques which are commonly

used for geotechnical site investigation include seismic reflection and refraction (Cook 1965; Steeples and Miller 1987), seismic surface waves (Ismail and Anderson 2007), ground-penetrating radar (Ballard 1983 and Annan et al. 1991) and electrical resistivity tomography (Griffiths and Barker 1993; Zhou et al. 2002; Roth et al., 1999; Labuda and Baxter 2001 and Ahmed and Carpenter 2003). These geophysical techniques can precisely map a buried bedrock surface, depth to the groundwater table as well as lateral and vertical variation of the soil properties at geotechnical sites.

This study was designed to characterize the upper 15 m of soils in the area surrounding the City Star shopping mall in the center of Cairo, Egypt. To the west of the mall, two buildings (No. 17 and No. 18) were contiguously built in the 1950s at the intersection of the Makram Ebaid extension and Mosque Street. During the past two years, it was noticed that building No. 17 was tilted and a displacement between this building and the adjacent building No. 18 was observed, especially the upper part. This structural defect has raised the concern about a possible collapse of the whole building if the tilting continues at the same rate. A group of civil engineers have reviewed the building design and construction to determine the reason of this tilting, and following a detailed study, the engineers found no design or construction problems that could cause such a tilting. The engineers recommended testing the upper 15 m of the soils underneath and surrounding the building foundations to locate voids, sinkholes, dissolutions and or lateral variation in the subsurface soils that could lead to instability beneath the building. A few boreholes were drilled surrounding the building to examine the soil profile at the site. However, the drilled boreholes were limited in number and in depth of penetration due to the high cost of drilling and the hazard that a big drilling rig could cause to the building. Therefore, geophysics was recommended as a non-invasive tool to characterize the subsurface soil surrounding the building.

In this study we utilized three geophysical techniques including multi-channel analysis of surface wave (MASW), ground penetrating radar (GPR) and electrical resistivity tomography (ERT) to characterize the upper 15 m of the subsurface surrounding buildings No. 17 and No. 18 with empha-

size on the tilted building (No. 17). The MASW method is designed to measure 1D and 2D shear wave seismic velocity profiles to depths on the order of 15 m. The shear wave velocity indicates soil stiffness, which helps in mapping the bedrock surface and in qualitatively describing the strength of the soil. These parameters are directly related to the ability of the soil to bear a structural load and they are usually estimated prior to most construction operations. The GPR technique measures the propagation velocity and reflection amplitude of the electromagnetic waves across the surveyed area. Measuring these parameters makes the GPR a powerful technique in imaging lateral and vertical variations in the soil type, mapping depth to the ground water table and locating the possible subsurface voids, sinkholes or cavities. The ERT technique measures variation in the soil electrical conductivity indicating the variation in the soil type, porosity, moisture and clay content. Integrating the results from these three geophysical techniques, MASW, GPR and ERT, are expected to sufficiently characterize the subsurface surrounding the building and reveal the reasons behind the tilting of the building.

## 2. Site description

The investigated site is located along the eastern bank of the Nile River in one of the most densely populated areas of Cairo, Naser City Fig. 1.

The site under consideration comprises two buildings (Nos. 17 and 18) shown in Fig. 2. Almost, half of the site was designated to the building, while the rest of the site was used as parking lots. The eastern and northern sides of the site face two high traffic flow streets due to the presence of the City Star mall. The western and southern sides face two narrow low-flow traffic streets. Building No. 17 started to show tilting at its NE section during the past few years (Fig. 3) and was recently evacuated. None of the other buildings in the region near the investigated site showed any signs of tilting or similar structural or geotechnical problems. Also, the investigated site is not close to any mining activities, railway tracks or other source which may have resulted in shaking and tilting of the building.

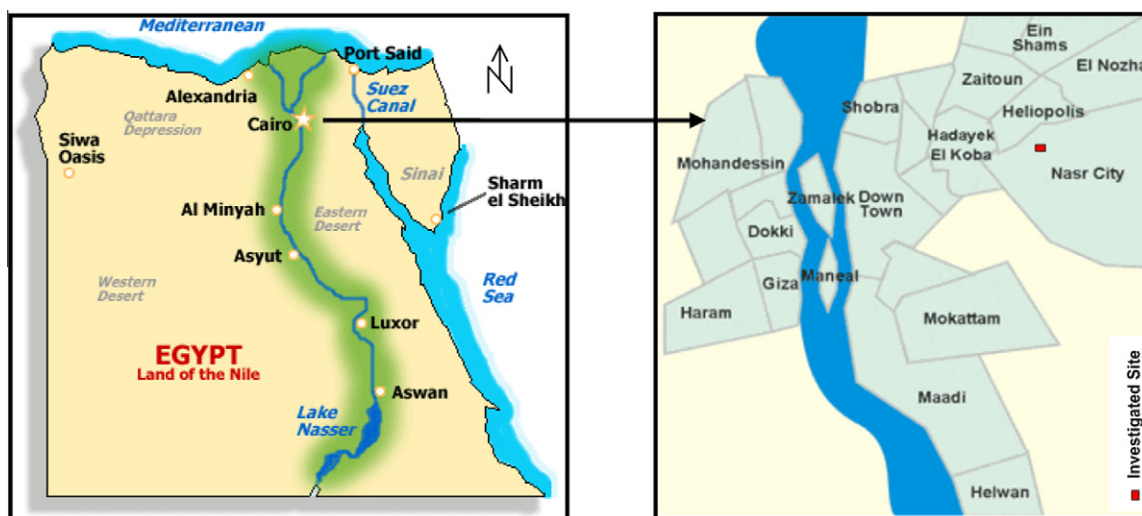
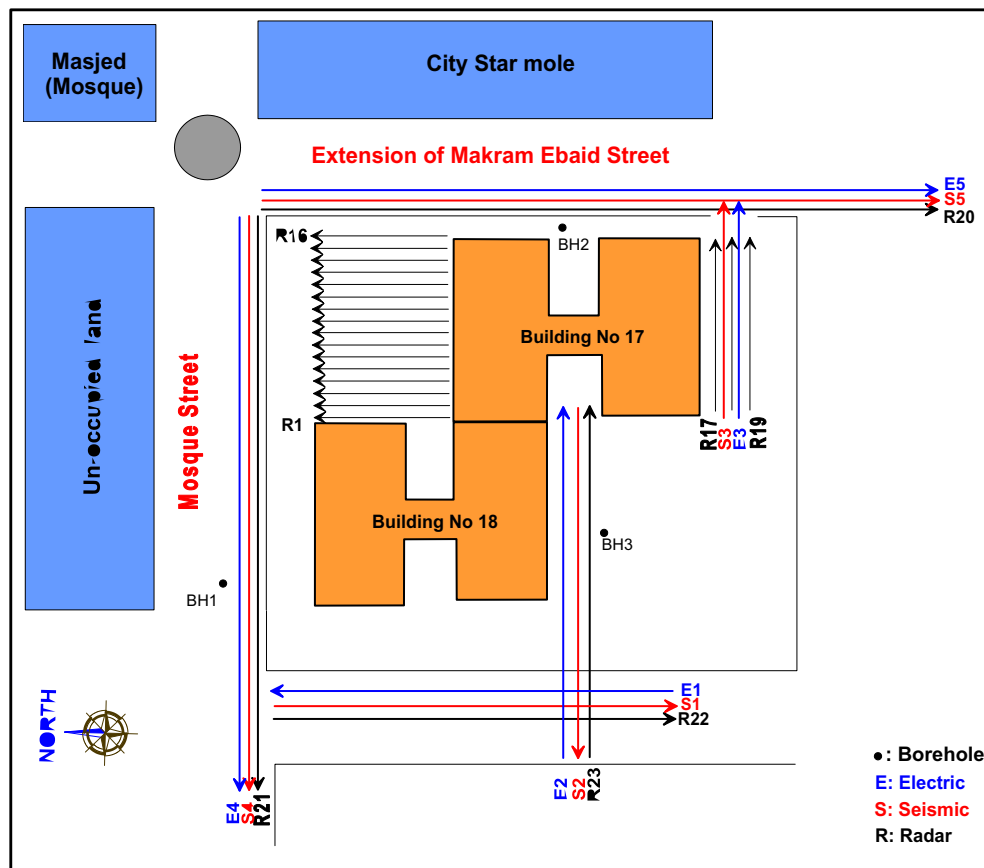


Figure 1 Location map of Naser City including the investigated site (not scaled).



**Figure 2** Location map of the investigated site showing the distribution of the geophysical surveys over the site. The black lines represent the GPR profiles, the red lines represent the MASW profiles and the blue lines represent the 2D ERT profiles.

### 3. Geological setting

Swedan (1991) stated that the oldest rocks exposed in the Greater Cairo area are those occupying the anticlinal structure of Abu Rawash. He added that the structural pattern of the Greater Cairo area is mainly controlled by faults and folds. The main fault systems are trending NW–EW (Eriethrean and Tethyan trends). The area of Greater Cairo is covered by sedimentary rocks of different formations from the Eocene up to the Quaternary (El Shazly et al., 1980), as shown in Fig. 4.

The tilted building resides on the flood plain of the Nile River that consists of alternating thin beds of cemented silty sand, clayey sand and medium to coarse sand (Sabry 1989). These sediments were deposited by the river in its valley on the surface of the Eocene Limestone bedrock (Said 1981). The flood plain sediments changes laterally over small areas from graded-sized consolidated sand, to clayey sand, to silty sand and to clayey silt. The description of the uppermost 15 m of soil is shown in Table 1 based on the boring information from the three boreholes drilled at the investigated site in 2009 by the Cairo University Engineering Center.

The ground water table at the site was measured in some test holes in the area in 1989 to be 5.0 m below the ground surface. It was also measured in 2009 and it rose slightly at the site. Therefore, the rising groundwater table is definitely at least one factor responsible for affecting the properties of flood plain sediments at the site. However, it was not determined if this rise in the groundwater table was due to a regional change in the ground

water table or due to a local effect such as the recently discovered leakage from sewage and drinking water pipes in the area.

### 4. Geophysical data acquisition and processing

#### 4.1. GPR survey

A total of 23 GPR profiles were conducted surrounding building No. 17 as shown in Fig. 2, with different lengths according to the validity of the scanned area. The GPR data were acquired using an SIR 3000 system by GSSI equipped with a 400 MHz antenna. The data were acquired in continuous mode with a time sampling interval of 512 and a time window of 140 ns.

The GPR data were processed using programs RADAN 6.5 and REFLEX 5.0 to remove the noise signal and to enhance the imbedded features' signals. Several processing steps were applied including;

- (1) Static correction for the ground zero level,
- (2) Background removal to facilitate the recognition of the imbedded infra-structure,
- (3) Band-pass 2D filter to remove the noise and get clear sections, and
- (4) An automatic gain control (GC).

The velocity used for time/depth conversion was estimated by performing GPR over the known buried water, sewer, and other pipes at the site.





**Figure 3** Tilting of Building No. 17 relative to Building No. 18.

#### 4.2. MASW survey

The MASW was acquired along five linear traverses totaling 240 m surrounding the tilted building using twelve, 14-Hz low-frequency geophones spaced at 1–2 m intervals. A 10-kg hammer was used as a source and was fired at a 2 m distance from the first geophone. The source and the geophones were

moved at 6 m intervals. This recording geometry was sufficient to provide shear wave velocity information between a depth of 1 and 15 m. Because the entire survey site was covered with asphalt, the geophones were attached to concrete plates so that adequate coupling could be achieved between the geophones and the ground. Each of these concrete plates had a central hole where the geophone spike was planted in and supported

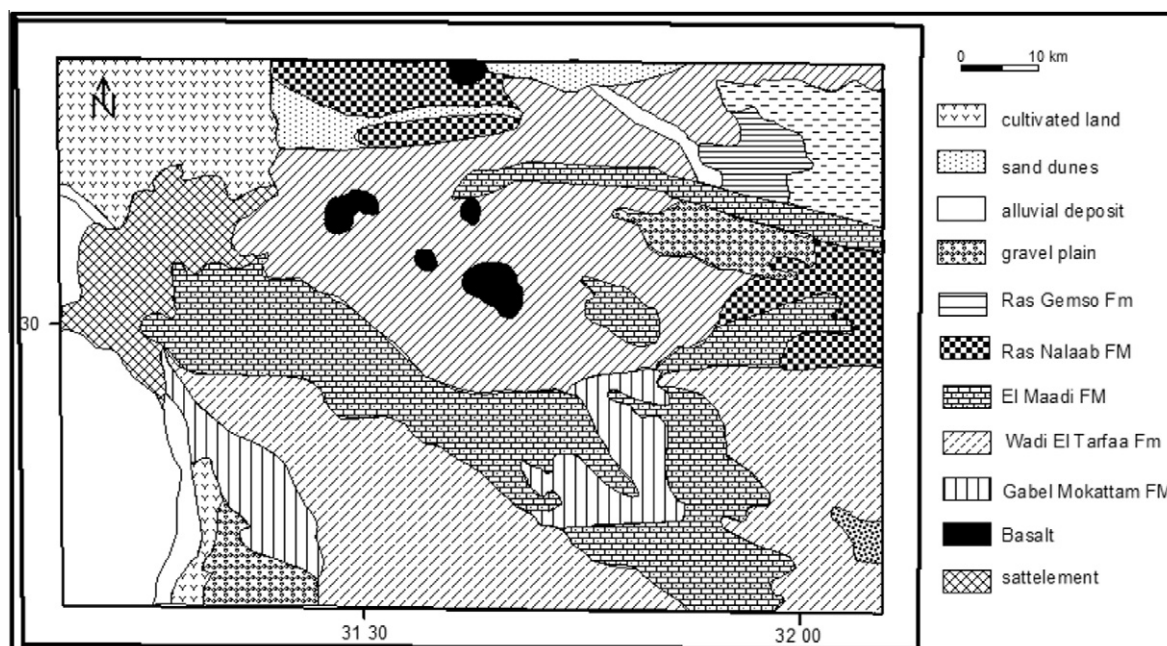


**Figure 4** Geological map of Greater Cairo area (El Shazly et al., 1980 & Williams and Small, 1984).

**Table 1** Lithologic description obtained for the investigated site based on 3 boreholes (15 m depth).

| BH1  | BH2  | BH3  |
|--|--|--|
| 0–2 m: trial pit no. 1                         | 0–2.5 m: trial pit no.2  | 0–1 m: pre-exacted for utilities                                       |
| 2–4 m: clayey sand and sandstone with gravel   | 2.5–6 m: silty clayey sand with gravel, concrete and cemented sand fragments | 1–9 m: silty sand, gravels.  |
| 4–7.5 m: calcareous gravelly clayey sand, silt | 6–6.5 m: calcareous silty clay and sand                                      | 9–9.5 m: weak to moderately hard sandstone                             |
| 7.5–9 m: silty clay                            | 6.5–15 m: calcareous gravelly clayey sand                                    | 9.5–15 m: calcareous gravelly clayey sand with thin layer of sandstone |
| 9–15 m: slightly cemented silty clayey sand    |  |  |

by soft clay (Fig. 5). The acquired data were not of high quality due to the location of the surveyed site in the center of the heavily populated area. Cultural noise from traffics, pedestrians, power lines and other sources generated noise in the recorded shot gathers.

The acquired MASW shot gathers along the lines consisted of 12-traces of 1 s trace length and sampled at 1 ms sampling intervals with no frequency filters applied during data acquisition. These multi-channel records were analyzed with the Surf-Seis software package of the Kansas Geological Survey, using the MASW method. During data analysis, each shot gather was transformed from time domain into frequency domain using the Fast Fourier Transform approach (Park et al., 1999). Each transformed shot gather was used to generate a site-specific dispersion curve (a plot of phase velocity versus frequency). A 1-D shear-wave velocity ( $V_s$ ) profile was calculated from the dispersion curve of each shot gather using an iterative non-linear inversion process (Xia et al., 1999). The inversion method uses a starting model before beginning to search for the answer in an iterative manner. The starting model consists of several key parameters: S-velocity ( $V_s$ ), P-velocity ( $V_p$ ), density ( $\rho$ ), and thickness ( $H$ ) of the layers in the earth model. Using this set of parameters, the program begins searching

for a solution, continuously converging on the most probable values.  $V_s$  is the parameter that is the most sensitive and influential to the surface wave phase velocity. The influence of all other parameters can usually be neglected as long as they have been reasonably estimated. The shear-wave velocity profiles derived from all the shot stations along the surveyed line were interpolated using a Kriging algorithm. The generated 2-D grid was color contoured to produce a 2-D profile plot.

#### 4.3. ERT survey

Resistivity imaging surveys (Fig. 6) measure variations in the electrical resistivity of the ground in the vertical direction, as well as in the horizontal direction along the survey line, by applying small electric currents across arrays of ground electrodes. The survey data are processed to produce graphic depth sections of the thickness and resistivity of subsurface electrical layers. The resistivity sections are correlated with ground interfaces such as soil and fill layers or soil–bedrock interfaces, to provide engineers with detailed information on subsurface ground conditions. The 2-D resistivity images obtained with such multi-electrode technique are used for locating resistivity anomalies. Resistivity imaging which is also





**Figure 5** Acquisition processes of the MASW data using geophones attached to concrete plates and the ERT data where long steel electrodes were used to penetrate the asphalt down to the conductive soil layer underneath the asphalt.

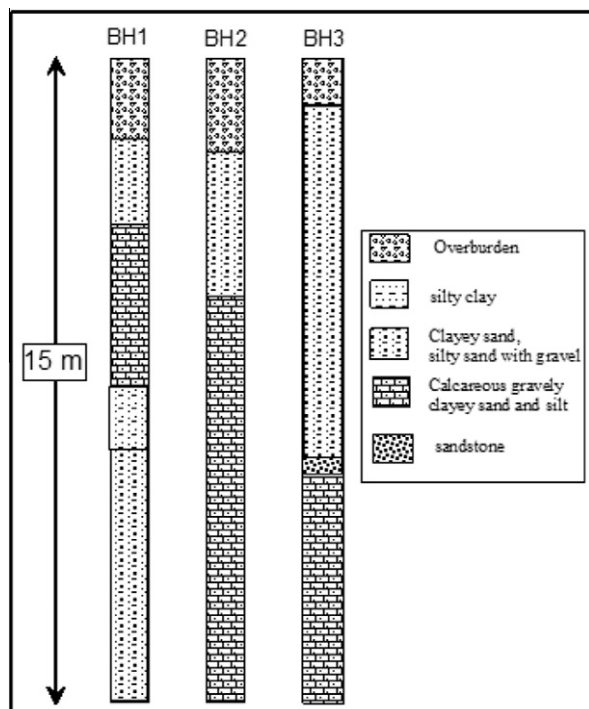


**Figure 6** Lithological log of the boreholes BH1, BH2 and BH3.

known as electrical resistivity tomography (ERT) is particularly useful in clayey ground where methods such as Ground Penetrating Radar (GPR) are less effective. The method helps to define transitional boundaries which can be difficult to detect using other geophysical methods.

## 5. Data interpretation

### 5.1. GPR profiles

Four representative GPR profiles are shown in Figs. 7–10. The GPR profiles show three distinct layers. The upper layer has a thickness ranging from 0.5 to 1 m and is characterized by coherent strong GPR reflections. This upper layer most likely corresponds to the asphalt layer that covers the entire survey site. Directly below the asphalt layer is a second thin layer (0.5 m thickness) that is relatively weak and less coherent compared to the reflections of the overlying asphalt layer. This second layer most likely corresponds to a layer of fill materials beneath the asphalt. A third layer was identified on all the GPR profiles at depths ranging from 1 to 2 m and extends to the maximum depth of the GPR profiles. Reflections in this layer become much weaker and less coherent with depth, which is most likely due to the relatively higher moisture content within the materials of this layer.

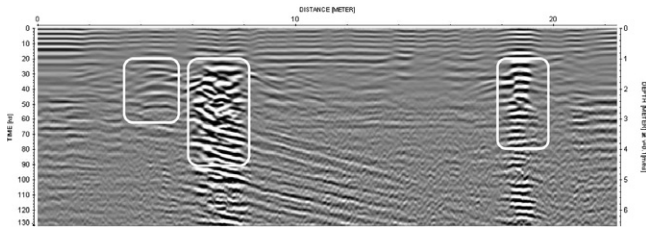


Figure 7 GPR profile R4.

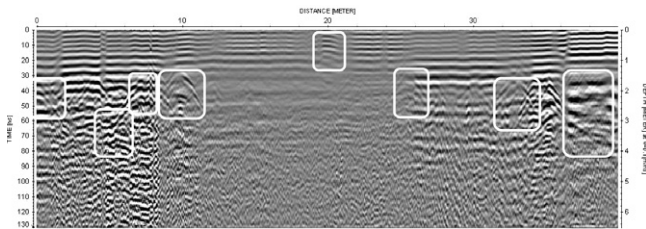


Figure 8 GPR profile R19.

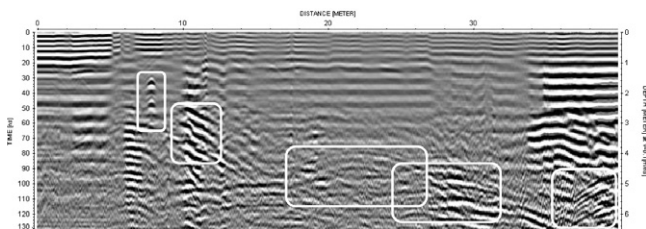


Figure 9 GPR profile R20.

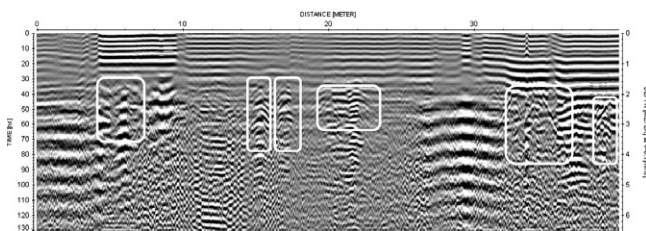


Figure 10 GPR profile R22.

The lateral variation in the GPR reflection strength along the GPR profiles, may be due to water mass accumulations resulting from seepage from water lines and/or sewer pipes, these zones are marked with the white-lined squares on GPR sections. For example the middle sections of GPR profiles 19 and 20 (Figs. 8 and 9) show much weaker GPR reflections compared to those at the sides of the same profiles. Such a severe lateral variation in the GPR reflection over short distance could be related to either variation in the soil moisture or clay content. Such variations will definitely have some effect on the strength of the soil underneath and below the foundation of the building.

5.2. Seismic profiles

Locations of the seismic profiles are illustrated in Fig. 2. The lengths of these profiles range from 50 m to 70 m. Prior to processing the seismic profiles to generate shear wave velocity

profiles, the first arrivals were picked and then inverted using the seismic refraction tomography method. The produced P-wave velocity profiles are displayed in Fig. 11. The seismic tomography sections show two P-wave velocity layers; a shallow low-velocity layer that has a velocity ranging between 300 and 500 m/s and a thickness ranging between 1 and 2 meters; this

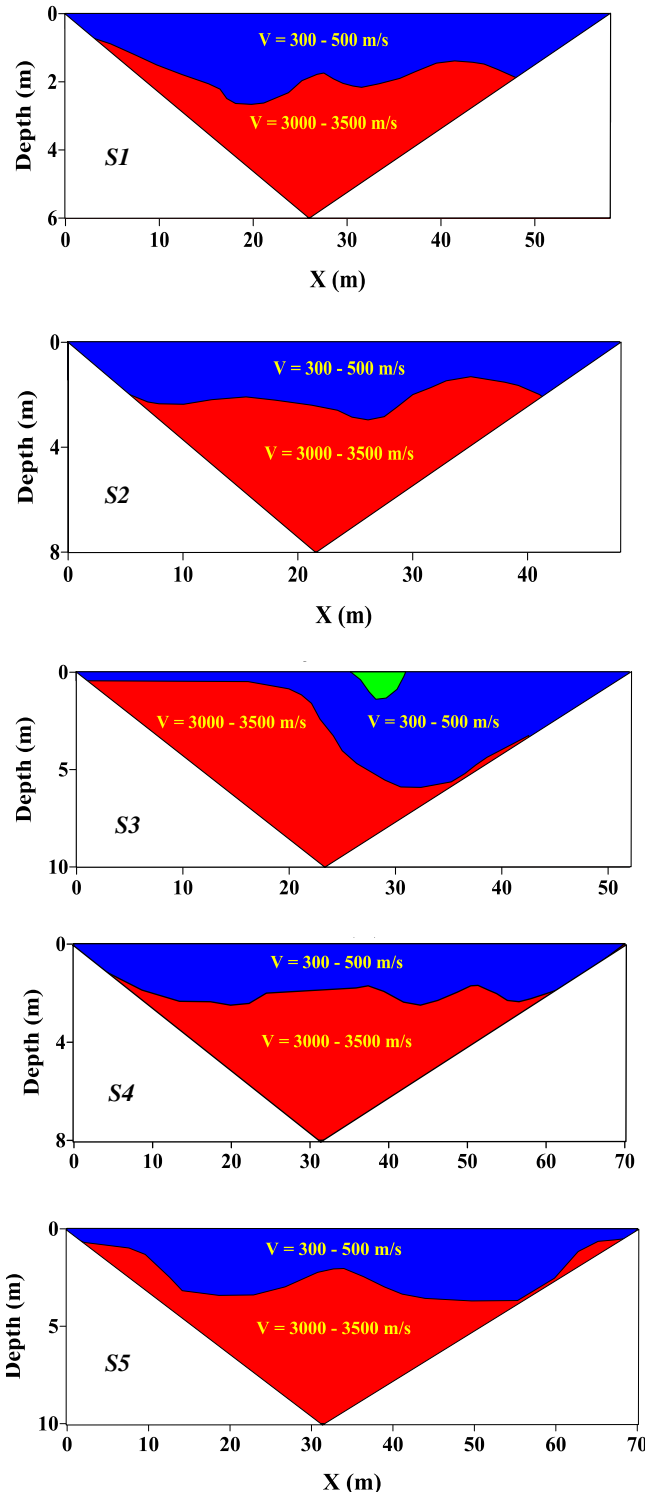


Figure 11 Seismic tomography sections of profile Nos. S1-S5.



layer corresponds to the uppermost weathered soil and attains a maximum thickness of 5 m along profile S3. The second layer has a velocity ranging between 3000 and 3500 m/s that correspond to coherent soil. Unfortunately, the seismic tomography tool divides the geological sections into only two velocity layers.

Three representative MASW profiles are shown in Fig. 12. The MASW profiles show the shear wave velocity distribution from the ground surface down to a maximum depth of 20 m. The shear wave velocity is a direct indication of the soil rigidity and its bearing capacity (Kramer, 1996). Low shear wave

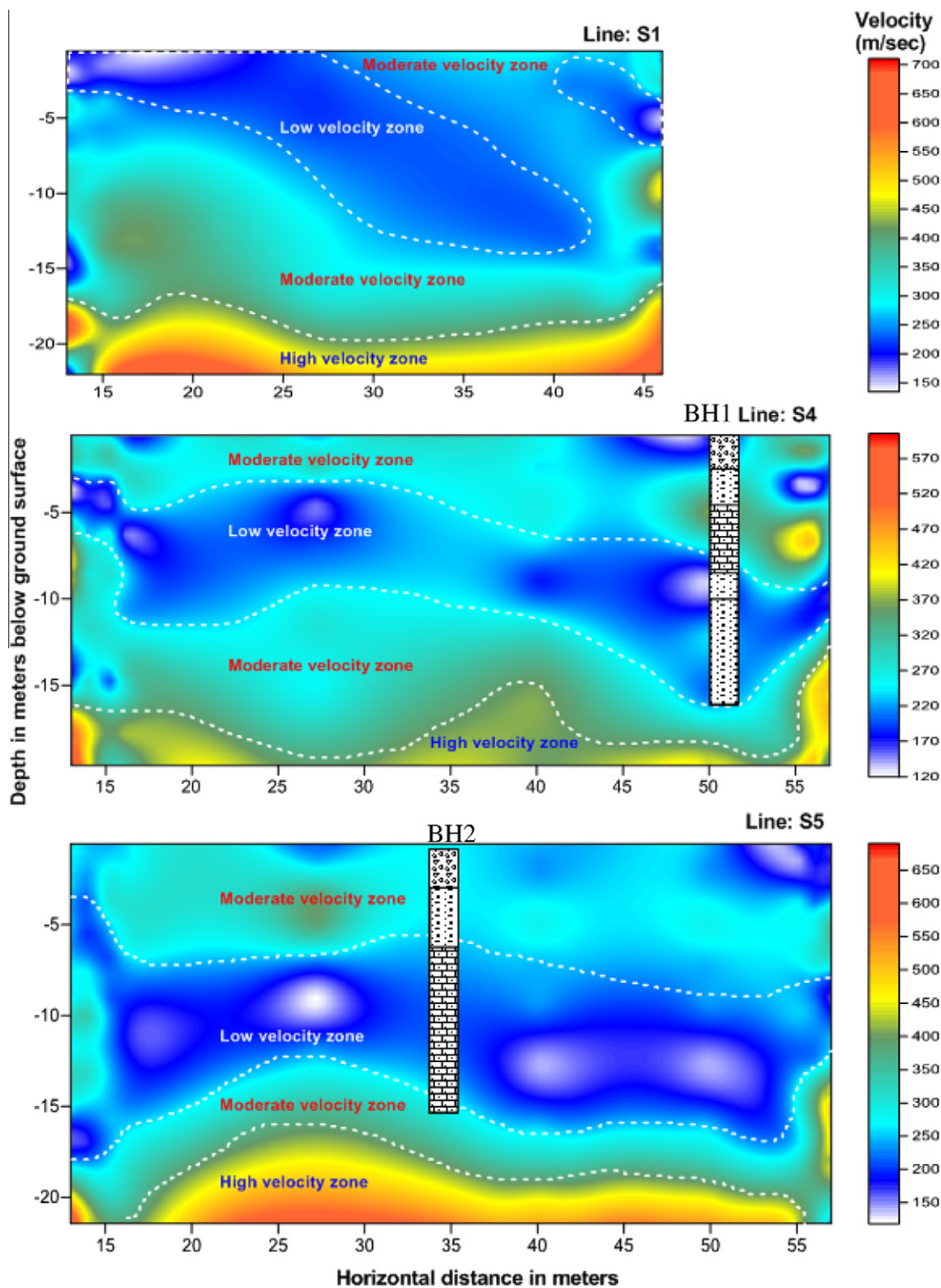


Figure 12 Three representative MASW profiles S1, S4 and S5 with the interpretation superimposed on the profiles.

velocity corresponds to a low rigidity of the soil and vice versa. Therefore, the shear wave velocity layers are interpreted as layers of different soil rigidity along the MASW profiles (Fig. 12). The rigidity distribution along the MASW profiles shows vertical and lateral variations. Generally, most of the MASW profiles show three layers of different soil shear wave velocity rigidity. The upper layer which starts at the ground surface and extends down to an average depth of 5 m shows relatively high shear wave velocity. The upper layer is underlain by a second layer of relatively low shear velocity and a variable thickness ranging from 3 to 9 m. A third layer of relatively high shear wave velocity is at the bottom of the MASW profiles.

The presence of a low shear wave velocity layer at an average depth of 5 m at the investigated site raises concern about the soil's shear strength below and in the vicinity of the building foundations. Moreover, the lateral variation in the values of the shear wave along the MASW profiles and the second layer of low shear wave velocity in particular indicates that the rigidity or the bearing capacity of the soil varies significantly across the area surrounding the tilted building (Fig. 12). Therefore, this may explain the reason behind the tilting of the building.

### 5.3. ERT profiles

Generally the ERT profiles (Fig. 13) show two distinct layers. The upper layer starts from the ground surface and extends down to a depth of 3–10 m. This layer is characterized by rel-

atively low resistivity which most likely corresponds to a higher clay- or moisture content soil. The lower layer is characterized by relatively high resistivity which reflects the presence of clay soil which varies in its lateral and vertical extents. The thickness of the low resistivity zone has the lowest value at profile E1 to the west of the building. Profile E2 (south of the building) shows low resistivity zone thickness that change from 5 to 10 m. The other two profiles #4 and #5 (north and east of the building, respectively) show the maximum occurrence of low resistivity zone with a thickness of 10–15 m. This result indicates that the foundation of the building has been rooted in the low resistivity zone corresponding to heterogeneous sediments (clay with intercalations of sand and gravel).

## 6. Discussion and conclusion

The GPR data show two layers of distinct electric properties; an upper layer 2 m thick that hosts various utilities, and a second layer representing old soil or more consolidated materials that extend to 5 m depth. No water seepage from the utilities of the building was observed on the surface during the present survey. However, the variation in the GPR reflectivity with depth may indicate water leakage from the sanitary system in the area (City Stars, public sewage system, etc.).

The electric resistivity imaging (ERT) and the seismic survey (MASW) results both showed comparable sub-surface soil

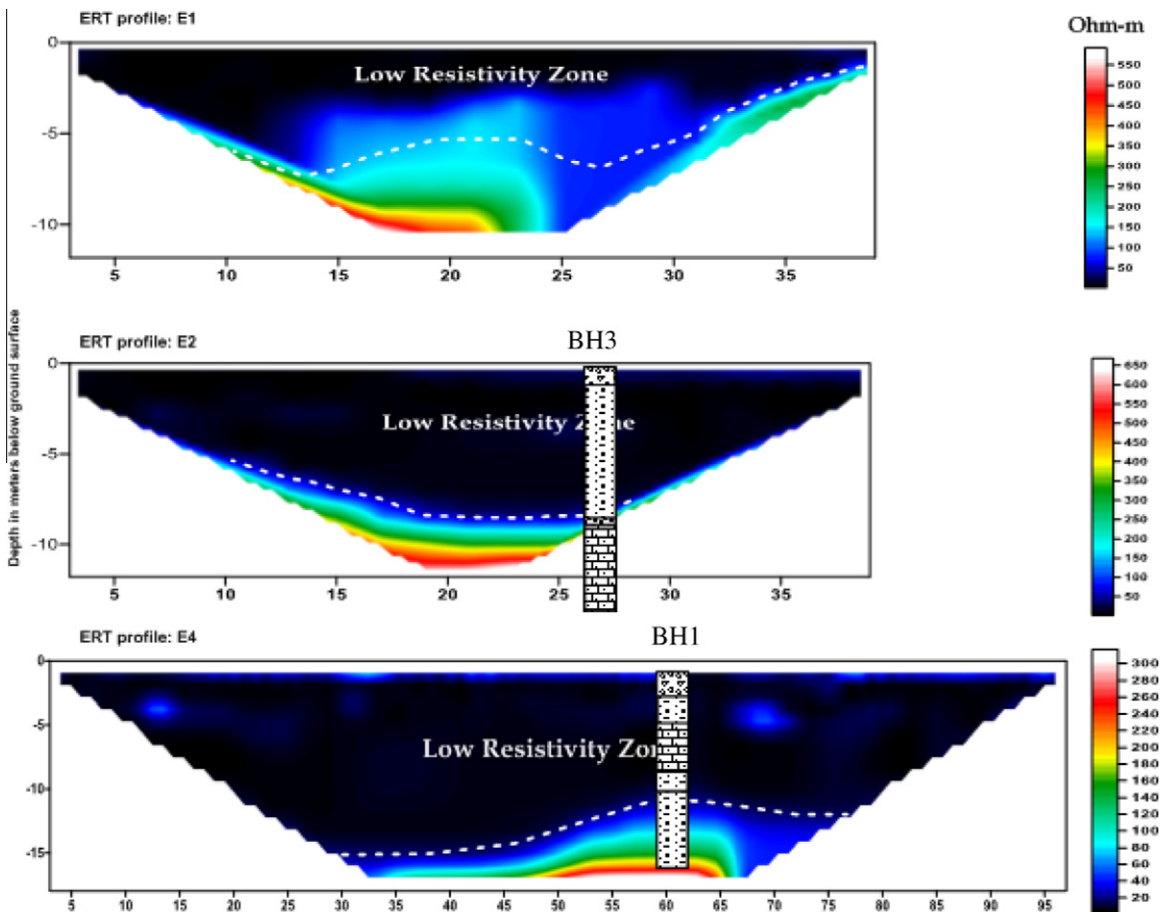


Figure 13 Three representative ERT profiles E1, E2 and E4 with the interpretation superimposed on the profiles.

conditions. Integrating the interpretation of the MASW and the ERT images with the boring information showed that the dominant soil within the upper 15 m is clay to silty clay with sand intercalations. This is underlain by sandstone intercalated by clays or silt to a depth of 25 m. The thickness of the upper layer from the ERT and MASW sections varies from line to line as described above. In addition to variations in thickness, variations in resistivity and shear wave velocity within the upper layer indicate that the subsurface soil is heterogeneous and varied in its rigidity (bearing capacity) and its compaction. Based on the rigidity retrieved from the MASW, the bearing capacity is not uniform in the area of the building.

The building foundation, at 3 m depth, was not excavated to the geophysical bedrock surface but rather was finished to cement, silty graded sand to sandstone, traces of gravel (from boreholes). Results from this investigation indicate that the upper 10 m has very low shear wave velocity and can easily shear under any load. The bearing capacity is directly related to shear wave velocity (Vaid and Chern, 1983; Kramer, 1996), which means that the lower the shear wave velocity the lower is the bearing capacity. Therefore, if, lower bearing capacity soils are present at some corners but not at the other corners foundation failure can occur and tilting of the building can be the result. The inspection of seismic lines S2, S3 and S5, shows a weak zone at the eastern and the southern sides of the building, extended to a depth below the foundation level. This weak zone has a low resistivity indicating either the existence of high moisture content, the presence of clay or most likely both. Similarly, a shallow weak zone exists at the northern and western sides of the building (seismic lines S4 and S1), but the soil is more rigid. Therefore, this asymmetry in the rigidity also likely contributes to the tilting of the building.

Finally, the soil surrounding and beneath the foundation of building 17 apparently was stable at the time of construction. However, various human impacts resulted in a change in its stability over time. These impacts include major construction operations for City Star mall and the surrounding buildings and leaking water from sewer pipes that increased moisture contents and may cause a subsequent dissolution in the subsoil. All of these are probable factors responsible for the instability of the subsoil and leading to variations in the bearing capacity at the corners of building 17 causing, shearing of the building, and its tilt.

### Acknowledgment

We acknowledge R. Berg, and D. Keefer, Illinois State Geological Survey, University of Illinois at Urbana-Champaign, USA for their thorough review of the manuscript.

### References

- Ahmed, S., Carpenter, P.J., 2003. Geophysical response of filled sinkholes, soil pipes and associated bedrock fractures in thinly mantled karst, east-central Illinois. *Environmental Geology* 44, 705–716.
- Annan, A.P., Cosway S.W., Redman, J.D., 1991. Water table detection with ground-penetrating radar. In: *Soc. Explor. Geophys. (Annual International Meeting Program with Abstracts)*, pp. 494–497.
- Ballard, R.F., 1983. Cavity detection and delineation research. Report 5, Electromagnetic (radar) techniques applied to cavity detection. Technical Report GL, 83–1, p. 90.
- Cook, J.C., 1965. Seismic mapping of underground cavities using reflection amplitudes. *Geophysics* 30 (4), 527–538.
- El Shazly, E. M., El Ghawaby, M. A., Salman, A. B., Khawask, S. M., El Amin, H., El Rakaiby, M. M., El Aassy, I. E., Abd El Megid, A. A., Mansour, S. I., 1980. Geological Map of Egypt. Remote Sensing Center, Academy of Scientific Research and Technology, Cairo, Egypt.
- Griffiths, D.H., Barker, R.D., 1993. Two-dimensional resistivity imaging and modeling in areas of complex geology. *Journal of Applied Geophysics* 29, 211–226.
- Ismail, Ahmed., Anderson, Neil., 2007. Near surface characterization of a geotechnical site North East Missouri using shear wave velocity measurements. *Near Surface Geophysics Journal, European Association of Geoscientists & Engineers* 6, 331–336.
- Kramer, Steven L., 1996. *Geotechnical Earthquake Engineering*, Prentice Hall, p. 653.
- Labuda, Z.T., Baxter, C.A., 2001. Mapping karst conditions using 2D and 3D resistivity imaging methods. In: Powers, M., (Ed.) *Proceedings of the Symposium on the Application of Geophysics to Engineering and Environmental Problems, Environmental and Engineering Geophysical Society, CDROM, Paper GTV-1*.
- Park, C.B., Miller, R.D., Xia, J., 1999. Multichannel analysis of surface waves (MASW). *Geophysics* 64, 800–808.
- Roth, M.J.S., Mackey, J.R., Mackey, C., Nyquist, J.E., 1999. A case study of the reliability of multi-electrode earth resistivity testing for geotechnical investigations in karst terrains. In: Beck, B.F., Pettit, A.J., Herring, J.G., (Eds.) *Proceedings of the 7th Multidisciplinary Conference on Sinkholes and the Engineering and Environmental Impacts of Karst, Balkema*, pp. 247–252.
- Sabry, A., 1989. *Drilling and Geotechnical investigation for the area near to City star Mall, Nasr city, Cairo, Egypt*. Ali Sabry Consulting Office, Internal Report.
- Said, R., 1981. *The geology Evolution of the river Nile*. Springer-Verlag, Newyork Heidelberg, Berlin.
- Steeple, D. W., Miller, R. D., 1987. Direct detection of shallow subsurface voids using high-resolution seismic reflection techniques. In: Beck, B. F., Wilson, W. L., Balkema, A. A., (Eds.) *Karst Hydrogeology: Engineering and Environmental Applications*, pp. 179–183.
- Swedan, A.H., 1991. A note on the geology of Greater Cairo area. Egyptian mineral resources authority. *Ann. Geol. Survey Egypt* 17, 239–251.
- Vaid, Y.P., Chern, J.C., 1983. Effect of static shear on resistance of liquefaction. *Soils and Foundations* 23 (1), 47–60.
- Williams, G. A. Small, J. O., 1984. A study of the Oligo-Miocene basalt in the Western Desert. In: *Proc. Petrol. Explo. Seminar, EGPC, Cairo*, pp. 252–268.
- Xia, J., Miller, R.D., Park, C.B., 1999. Estimation of near-surface shear-wave velocity by inversion of Rayleigh wave. *Geophysics* 64, 691–700.
- Zhou, W., Beck, B.F., Adams, A.L., 2002. Effective electrode array in mapping karst hazards in electrical resistivity tomography. *Environmental Geology* 42, 922–928.